Optik 127 (2016) 5738–5742

Contents lists available at ScienceDirect

Optik

journal homepage: www.elsevier.de/ijleo

Original research article

A novel chiral nano structure for optical activities and negative refractive index☆

Xiuli Jia, Qingxin Meng, Chengxun Yuan, Zhongxiang Zhou, Xiaoou Wang*

Harbin Institute of Technology, Harbin 150001, China

ARTICLE INFO

Article history:
Received 20 January 2016
Accepted 29 February 2016

MSC:
00-01
99-00

Keywords:
Metamaterial
Nanomaterials
Chiral
Optical activities
Negative refractive index
S-parameter retrieval method

ABSTRACT

In this paper, we present a chiral hollowed-out split ring resonators nano structure. This novel chiral nano structure can form multiple electric dipoles and magnetic dipoles in infrared and visible regions. And the interaction of these dipoles caused optical activities and multi-band negative refractive index. The appropriate geometric parameters are obtained through optimization and analysis of this structure. Circular dichroism, polarization azimuthal rotation angle, ellipticity, refractive index and chiral parameter are calculated using S-parameter retrieval method, and these optical properties can be tunable by the geometric parameters of the chiral structure. This chiral structure metamaterial would offer electromagnetic applications in the infrared and visible regions, for fields like imaging, invisibility cloak and perfect lensing.

1. Introduction

Electromagnetic (EM) metamaterials (MMs) are new fascinating artificial materials with ability to manipulate beams of light in surprising ways, this metamaterials with negative refraction have drawn much attention since Smith et al. successfully prepared such metamaterials in the laboratory in 2000 [1–11]. Chiral metamaterials with self-polarization and cross-polarization between electromagnetic fields can achieve a negative index of refraction depending on their chirality, whether or not the permittivity and permeability are negative. Furthermore, they can exhibit strong optical activity and lower loss of the electromagnetic wave (EMW) transmission [3]. The strength of cross-coupling is characterized by the chiral parameter ($\kappa = (n_+ - n_-)/2$), which is connected to the refractive index ($n_\pm = \sqrt{\varepsilon\mu} \pm \kappa$), ($n_{eff} = (n_+ + n_-)/2$), where ε and μ are the relative permittivity and permeability of the CCMs; n_+ and n_- represent the refractive indices of the right-handed circularly polarized (+, RCP) and left-handed circularly polarized (−, LCP) waves, respectively. At the same time, both RCP and LCP waves have the same impedance ($z = \sqrt{\varepsilon/\mu}$) [12].

Recently, negative refraction chiral metamaterials have shown large optical activities (e.g., $\theta = 130°$) [12], high frequency regions (3×10^{14} Hz) [13], lower loss (FOM = 4.2) [14], and high negative refraction value ($n = -180$) [15]. Chirality is the lack of the internal mirror symmetry of a molecule or artificial structure. Optical activity is a major characteristic of chiral metamaterials. In nature, optical activity is caused by the intrinsic spiral feature of chiral molecules or the spiral arrangement of its atomic molecules. The optical activity of a natural chiral medium is caused by the intrinsic helical characteristics of molecules or the spiral alignment of atoms, and the root of the rotation is circular birefringence, and strength is very weak. For artificial chiral metamaterials, optical activity is caused by the optical spatial dispersion of structural chirality. Compared with nature, chiral metamaterials have higher optical activities and chiralities [3,12,16–18]. Circular dichroism (CD, $\Delta = |T_{++}| - |T_{--}|$) refers to one of the main physical parameters for characterizing the absorption of the RCP wave and the LCP wave. The polarization azimuthal rotation angle ($\theta = (\arg(T_{--}) - \arg(T_{++}))/2$) refers to the angle of rotation with respect to the plane of polarization. The ellipticity ($\eta = \frac{1}{2}\arctan(\frac{|T_{++}|^2 - |T_{--}|^2}{|T_{++}|^2 + |T_{--}|^2})$) refers to the difference of polarization state of transmitted and incident waves, and also measures the CD effect. Here, T_{++} refers to the transmission coefficient of the RCP wave and T_{--} refers to the transmission coefficient of the LCP wave.

☆ This work was supported by the National Natural Science Foundation of China (No. 61205011) and the National Science Foundation of China (NSFC) (No. 61205093).

* Corresponding author.
E-mail address: wxo@hit.edu.cn (X. Wang).

http://dx.doi.org/10.1016/j.ijleo.2016.02.067
0030-4026/

In this paper, we used the finite difference time domain (FDTD) method to systematically study the negative refraction index (NRI) and optical activity. The geometrical parameters are optimized to show the strong optical activity, CD effect, and NRI at these resonance frequencies.

2. The structure design and mechanism analysis

We present a chiral structure based on a conjugated bilayer metal split-ring resonators, as shown in Fig. 1. The unit size of the chiral structure is $x = y = 500$ nm. This chiral metamaterial consists of three layers (i.e., Au/polyimide/Au). Babinets principle was applied to the design of the metamaterial, resulting in both a complementary spectral response and fields [19–22]. The metal layer thickness is represented by t, the dielectric layer thickness by d, the width of the ring by g (outer radius minus inner radius), and the angle of cut by α. The location of the cut rotates by 90° from ring to ring. The dielectric constant of the polyimide is 3.5, and the loss tangent is tan $\delta = 0.003$. Au can be described by Drude dispersion model as follows: $\varepsilon = 1 - \omega_p/\omega(\omega + i\omega_\gamma)$. The plasma frequency is $\omega_p = 1.37 \times 10^{16}\ s^{-1}$, and the collision frequency is $\omega_\gamma = 2.04 \times 10^{14}\ s^{-1}$ [23]. The back metal layer is obtained by rotating the front layer by 180° around the *Y*-axis.

In order to understand the NRI and optical activity mechanism of this chiral metamaterial, we investigate the current density distributions and electric field distributions at nine resonance frequencies, as shown by Fig. 2. For this chiral structure, strong coupling was found between each layer of metal, which formed symmetric and asymmetric current distributions on the surface of the metals. This also generated a strong coupling between the electric and magnetic field, as well as a large chiral parameter, thereby achieving negative refraction. The metal surfaces form multiple current density distribution areas are located inside and outside of the split rings, which can be divided into two regions: the parallel direction region, forming an electric dipole, and the anti-parallel direction region, forming a magnetic dipole, as shown in Fig. 2(a). This mechanism of resonance is different from that of the single electric or magnetic dipole of the cross chiral structure [24]. Thus, the multiple resonance frequencies are result from the interaction of multiple electric and magnetic dipoles. Interplay between the adjacent electromagnetic dipoles is an experimental priority in metamaterial design. It is an important factor determining the chirality of the structure, optical activities and negative refractive index.

The electric field strength distribution is calculated for well understanding the coupling enhancement mechanism. Fig. 2(b) depicts the electric field distribution with SRRs structures at (f_1 to f_9) 1.7378×10^{14} Hz, 2.3599×10^{14} Hz, 3.8499×10^{14} Hz, 4.3562×10^{14} Hz, 4.9638×10^{14} Hz, 6.2224×10^{14} Hz, 6.6854×10^{14} Hz, 7.0181×10^{14} Hz, and 7.3074×10^{14} Hz, respectively. We can see that the SRRs produce strong electric resonance and highly localized electric field energy at the gap is coupled

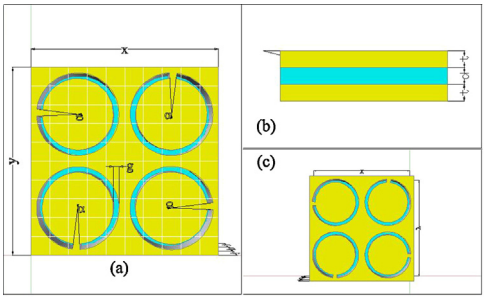

Fig. 1. The unit cell of the chiral metamaterial. (a) Front, (b) side, and (c) back.

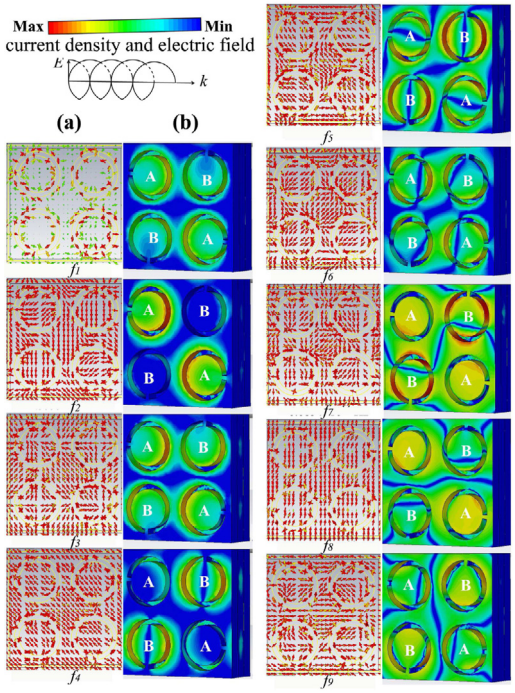

Fig. 2. (a) Distributions of the surface current density. (b) Electric field at nine resonance frequencies.

to the hole except the cut of SRRs. Besides, there is relatively rather strong resonance in SRR_A (the split rings of A), which contributes to the interaction of multiple electric and magnetic dipoles enhancement. The other enhancement is mainly due to the resonance of SRR_B (the split rings of B), as show in Fig. 2(b).

The electric field distribution of hollowed-out SRRs in this paper is much different from the traditional SRRs [15,24–26]. The traditional SRRs, which the electric field distribution focused on the splits, and most of the other place the electric field is almost zero. Inversely, the electric field of the hollowed-out SRRs is distributed on the gap of the SRRs. The intensity of electric field is stronger than the traditional structure obviously.

From Fig. 2(b), group SRR_A and group SRR_B have the same electric field distribution respectively, but group SRR_A is different with group SRR_B. The strength and weakness of the electric field distribution alternates from group A to group B. This is due to rotation of the electric field vector (E) of circular polarization wave in the plan of vertical wave vector (k) direction. With the increases of frequency, the interaction of coupling from metal film before polyimide and after is increases. The directions of splits are different before polyimide and after, but they have own distribution rule. With the increases of strengthen of the electric field, the interaction of coupling from metal film before polyimide and after is obviously. The electric field of before will be affected by after, and redistributes the electric field, appears more strong and weak areas. As shown the strongest electric field distribution areas of the group SRR_B from 1 (f_2), 2 (f_4) to 3 (f_7) in Fig. 2(b).

According to the S-parameter retrieve method, the effective EM parameters could be retrieved from the complex scattering parameters, i.e., S-parameters, include transmission T and refraction coefficients R [18]. The simulation has been performed based on the simulation software CST 2012. The periodic boundary conditions are applied to the x and y directions and the absorbing boundary conditions to the z direction as well. Based on above numerical simulation method, the final calculated S-parameters of multiple samples as shown by Fig. 3.